



Two-dimensional speckle tracking echocardiography detected interventricular dyssynchrony predicts exercise capacity and disease severity in pre-capillary pulmonary hypertension

Bing-Yang Liu^{1#}, Wei-Chun Wu^{2#}, Qi-Xian Zeng^{1#}, Zhi-Hong Liu¹, Li-Li Niu², Yue Tian², Xiao-Ling Cheng¹, Qin Luo¹, Zhi-Hui Zhao¹, Li Huang¹, Hao Wang², Jian-Guo He¹, Chang-Ming Xiong¹

¹Department of Cardiology, Pulmonary Vascular Disease Center, State Key Laboratory of Cardiovascular Disease, ²Department of Echocardiography, Fuwai Hospital, National Center for Cardiovascular Diseases, Chinese Academy of Medical Sciences and Peking Union Medical College, Beijing 100037, China

Contributions: (I) Conception and design: BY Liu, WC Wu, QX Zeng, CM Xiong; (II) Administrative support: CM Xiong; (III) Provision of study materials or patients: ZH Liu, LL Niu, Y Tian, XL Cheng, Q Luo, ZH Zhao, L Huang, H Wang, JG He; (IV) Collection and assembly of data: ZH Liu, LL Niu, Y Tian, XL Cheng, Q Luo, ZH Zhao, L Huang, H Wang, JG He; (V) Data analysis and interpretation: All authors; (VI) Manuscript writing: All authors; (VII) Final approval of manuscript: All authors.

[#]These authors contributed equally to this work.

Correspondence to: Prof. Chang-Ming Xiong. No.167 North Lishi Road, Xicheng District, Beijing 100037, China. Email: xiongcmfw@163.com.

Background: Right ventricular (RV) intraventricular mechanical dyssynchrony detected by two-dimensional speckle tracking echocardiography (2D-STE) has been reported to be correlated with a decrease in RV contractile efficiency in pulmonary hypertension (PH) patients, while little attention has been paid to biventricular dysfunction. Therefore, we aimed to evaluate the predictive value of 2D-STE detected interventricular dyssynchrony for exercise capacity and disease severity in patients with pre-capillary PH (PcPH).

Methods: Conventional transthoracic echocardiography, 2D-STE and cardiopulmonary exercise tests (CPETs) were performed in all participants. Intra- and interventricular dyssynchrony were calculated as the standard deviation (SD) of the time intervals corrected for heart rate between QRS onset and peak longitudinal strain. Multivariate linear regression analyses were performed to identify independent predictors of peak oxygen consumption (PVO_2) during the CPET. Multivariable logistical regression modeling was used to analyze the associations between interventricular dyssynchrony and risk assessment.

Results: Sixty-six PcPH patients were consecutively recruited (19 male and 47 female, average 35 years old). WHO functional class, N-terminal pro-brain natriuretic peptide (BNP) and body mass index were included as independent predictors in the first multivariate regression analysis of clinical data without echocardiographic parameters (Model-1, $r^2=0.423$, $P<0.001$). We subsequently added conventional echocardiographic parameters and 2D-STE parameters to the clinical data, RV fractional area change (Model-2, $r^2=0.417$, $P<0.001$), RV global longitudinal strain (Model-3, $r^2=0.454$, $P=0.001$), RV intraventricular dyssynchrony (Model-4: $r^2=0.474$, $P<0.001$) and interventricular dyssynchrony (Model-5, $r^2=0.483$, $P<0.001$) were identified as independent predictors of PVO_2 . Interventricular dyssynchrony, calculated as the SD of the time intervals of nine segments, was independently associated with risk assessment (odds ratio 1.027, 95% CI: 1.003–1.052, $P=0.03$). The area under the receiver-operating characteristic curve (AUC) was 0.73 ($P<0.001$).

Conclusions: Interventricular dyssynchrony detected by 2D-STE contributed to a better evaluation of exercise capacity and disease severity in PcPH patients.

Keywords: Pulmonary hypertension (PH); two-dimensional speckle tracking echocardiography (2D-STE); interventricular dyssynchrony; peak oxygen consumption (PVO_2); risk assessment

Submitted Dec 02, 2019. Accepted for publication Feb 11, 2020.

doi: 10.21037/atm.2020.03.146

View this article at: <http://dx.doi.org/10.21037/atm.2020.03.146>

Introduction

Pulmonary hypertension (PH) describes a group of disorders that cause pulmonary vascular remodeling and pulmonary artery pressure increase, which subsequently increases the afterload of right ventricle (RV) and ultimately leads to progressive RV failure (1). Pre-capillary PH (PcPH), defined as a pulmonary artery wedge pressure (PAWP) ≤ 15 mmHg and a pulmonary vascular resistance (PVR) > 3 Wood units (WU), includes pulmonary arterial hypertension (PAH), chronic thromboembolic PH (CTEPH) and PH due to other diseases, except left heart disease (1). It is well established that the progression of PH results in an increase of RV afterload and eventually systolic dysfunction of RV, simultaneously, left ventricular (LV) dysfunction has been gradually recognized by researchers, even in mild PH patients (2). The bilateral ventricles are anatomically and functionally coupled (3), and the dysfunction of one ventricle will inevitably affect the other. However, little attention has been paid to biventricular dysfunction in PcPH patients.

Impaired exercise capacity is one of the typical symptoms of PH, and it is often used to evaluate disease severity and prognosis as well as to determine the indication and opportunity for heart and/or lung transplantations (4,5). The 2015 European Society of Cardiology (ESC) Guidelines for the diagnosis and treatment of PH recommended that the basic assessment of PH patients include WHO functional class (WHO-FC) and exercise capacity, which is detected by a cardiopulmonary exercise test (CPET) or a six-minute walk test (6MWT) (6). Peak oxygen consumption (PVO_2), characterized by objective and digital appraisal of monolithic cardiopulmonary functions, is one of the most widespread CPET parameters used for therapeutic decision making (7,8). However, in patients with certain contraindications, such as uncontrolled symptomatic heart failure, CPET may be associated with procedural risks (9). Additionally, some of the indices of the 2015 ESC risk assessment strategy (6) were invasive, such as right heart catheterization (RHC). Therefore, we need safer and more convenient evaluation techniques for risk assessment of

PH patients, especially for those with absolute or relative contraindications to RHC or CPET.

As a low-cost, noninvasive and reliable tool, echocardiography is widely used to assess the structure and function of heart. Recent studies have shown that impaired RV longitudinal strain, strain rate and intraventricular mechanical dyssynchrony detected by two-dimensional speckle tracking echocardiography (2D-STE) were correlated with a decrease in RV contractile efficiency (10), impaired exercise capacity (11,12), invasive hemodynamic parameters (13) and worse prognosis (14,15) in PH patients without obvious electrical dyssynchrony, which was identified by QRS duration > 120 ms based on electrocardiography (ECG). Furthermore, simultaneous LV dyssynchrony was observed in patients with PH, quantified by STE imaging or cardiac magnetic resonance imaging (CMR) (16,17). We hypothesize that both inter- and intraventricular dyssynchrony may correlate with decreased exercise capacity. Therefore, we first proposed 2D-STE to detect interventricular dyssynchrony and investigated the predictive value of interventricular dyssynchrony for exercise capacity and risk assessment according to the 2015 ESC Guidelines in PcPH patients.

Methods

This is a single-center study from the Pulmonary Vascular Disease Center of Chinese Academy of Medical Sciences, Fuwai Hospital. Sixty-six patients diagnosed with PcPH according to the 2015 ESC Guidelines were consecutively enrolled from April 2017 to March 2018, the sample included 44 patients with idiopathic PAH (IPAH, 66.7%), 10 with CTEPH (15.2%), 8 with connective tissue disease induced PAH (CTD-PAH, 12.1%) and 4 with PAH after surgery for congenital heart diseases (6.1%). The exclusion criteria were as follows: (I) intracardiac right-to-left or left-to-right shunts; (II) QRS duration > 120 ms; (III) arrhythmia at the time of enrollment; (IV) significant left heart diseases or valve disorders; (V) acute heart failure; (VI) renal or hepatic failure; and (VII) other concomitant diseases, such

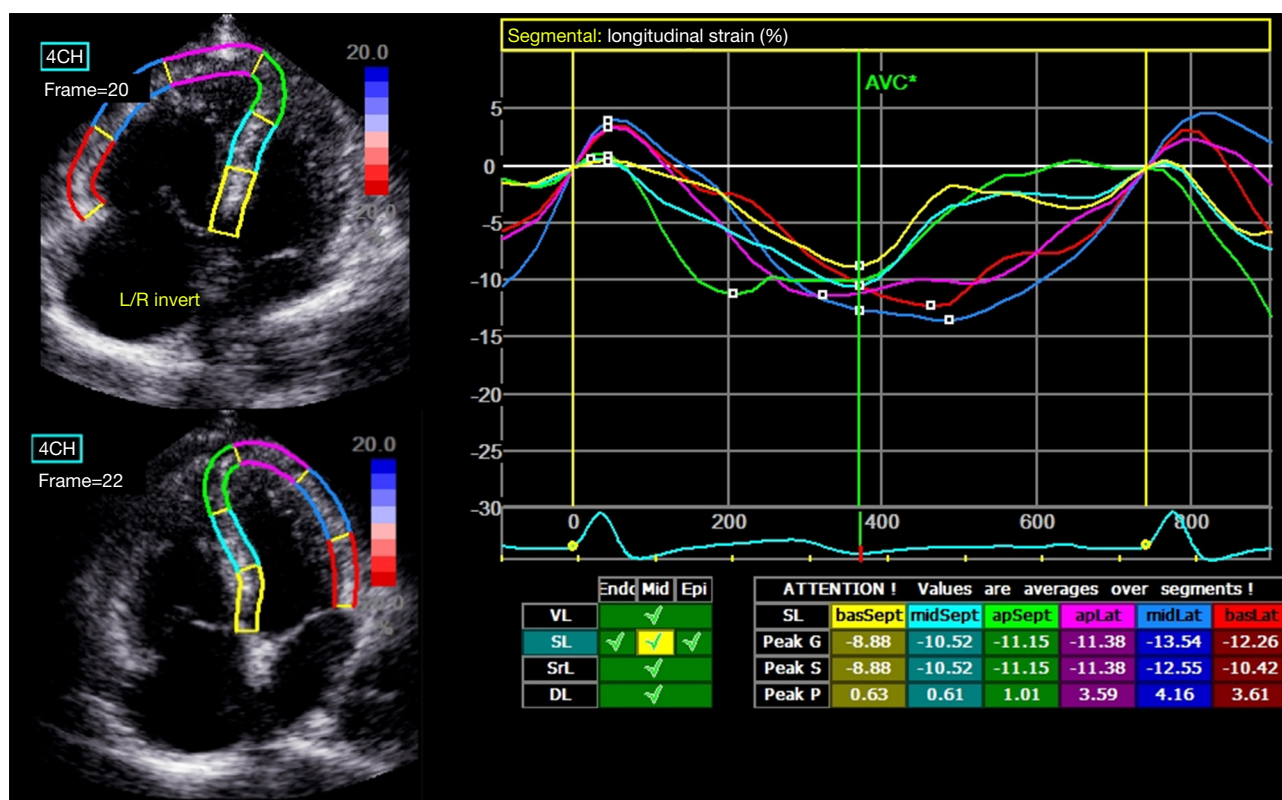


Figure 1 The RV and LV endocardial borders were traced and fine-tuned manually (left) and time-strain longitudinal curves of each segment were generated (right). The time intervals between QRS onset and peak longitudinal systolic strain were calculated for all RV/LV segments. RV, right ventricular; LV, left ventricular.

as hypertension and diabetes.

Standard transthoracic echocardiography was performed in 66 PcPH patients using Vivid S6 equipment (GE Medical Systems) with a 2.5- to 3.5-mHz probe by an experienced investigator. Standard M-mode, 2D and Doppler images were obtained from at least 3 consecutive beats. Then, GE EchoPAC version 201 was used to assess multiple parameters as follows: RV areas were measured from 2D imaging at two points—end ventricular systole, corresponding to end atrial diastole and identified as the frame just before tricuspid valve opening; and end ventricular diastole was identified as the point before the ventricular contraction, corresponding to end atrial systole. Then, the formula $(Area_{max} - Area_{min})/Area_{max}$ was used to calculate the RV fractional area change (FAC). Left ventricular ejection fraction (LVEF, 2D imaging), Doppler velocities of the trans-tricuspid flow (E, A), Doppler velocities of the tricuspid annulus (E', S', pulsed Doppler tissue image) and tricuspid annular plane systolic excursion (TAPSE, M-mode tracings) were measured

according to the guidelines of the American Society of Echocardiography (18).

Standard grayscale 2D images in 4-chamber and RV-focus 4-chamber views were obtained for speckle-tracking analyses using GE EchoPAC version 201, which required at least 3 consecutive beats and a frame rate >40 fps. The RV and LV endocardial borders were traced and fine-tuned manually to ensure that the six segments (basal, middle and apical of the free wall and interventricular septum) were tracked appropriately (insert *Figure 1*, left), then the time-strain longitudinal curves of each segment and RV global longitudinal strain (RV-GLS) were generated (insert *Figure 1*, right). The time intervals between QRS onset and peak longitudinal systolic strain were calculated for all RV/LV segments and corrected for heart rate according to Bazett's formula (19). RV intraventricular dyssynchrony was calculated as the standard deviation (SD) of the aforementioned corrected time intervals for the six segments of RV, referred to as RV-SD6, and LV intraventricular dyssynchrony (LV-SD6) was identified in the same way.

We calculated LV/RV interventricular dyssynchrony in two different ways because there were no standard definitions or measurements for 2D-STE identified interventricular dyssynchrony: (I) LSR-SD9: the SD of corrected time intervals of nine segments that contained six segments of the RV and three segments of the LV free wall; (II) LR-SD6: the SD of corrected time intervals of six segments including the left ventricle and the RV free wall, without the segments of the interventricular septum.

A symptom-limited CPET with a 10 W/min incremental cycle ergometer was performed in 66 patients, and PVO_2 and peak respiratory exchange ratio (RER) were measured breath-by-breath (COSMED Quark PFT Ergo, Italy). If the RER was greater than 1.1, we considered the test to be maximal. Medical records were reviewed to obtain other clinical information: age, sex, body mass index (BMI), WHO-FC, laboratory examinations, ECG, six-minute walk distance (6MWD), hemodynamics and targeted agents. Then, a comprehensive risk assessment was performed according to the 2015 ESC Guidelines, and patients were divided into a low-risk group and a moderate-to-high-risk group, which were scored as 1 and 2 points, respectively (6). The low-risk classification was considered when a patient met all the following criteria simultaneously: no progression of symptoms or syncope; the absence of clinical signs of right heart failure; WHO-FC I-II; 6MWD >440 m; PVO_2 >15 mL/min/kg; N-terminal pro-brain natriuretic peptide (NT-proBNP) <300 pg/mL; no pericardial effusion; RAP <8 mmHg; CI ≥ 2.5 L/min/m² and SvO₂ >65%. Among the 66 PH patients, 58 patients were treatment-naïve and the intervals between echocardiography and RHC were less than 24 hours. Coincidentally, irrespective of RHC parameters, other clinical data of the other 8 patients did not meet the criteria of low risk; therefore, these patients were not excluded from our study and were classified in the intermediate-to-high-risk group.

Continuous data are described as the mean \pm SD, and categorical data are expressed as counts and proportions. Comparisons between groups were performed with one-way ANOVA, while the homogeneity of variance was analyzed by the Levene test. Linear correlation analyses were used to evaluate the correlations between clinical data, echocardiography parameters, 2D-STE characteristics and PVO_2 , expressed as a Pearson correlation coefficient (*r*). Multivariate linear regression analyses were performed to identify the independent predictors of PVO_2 by a stepwise variable selection method with a significant level for entry of 0.1 and a significant level to remain of 0.05. Sixty-nine

variables were included in each linear regression analysis, and the appropriate sample size was supposed to be five-to-ten-times that of the variables; therefore, the sample size in our study was considered acceptable for our purpose. Four models were constructed: Model-1 was limited to clinical data. We subsequently added conventional echocardiographic variables and 2D-STE parameters, including RV/LV intra-/interventricular dyssynchrony and RV-GLS, to clinical data, and Model-2, -3 and -4 were constructed. Details for each model are described by the corresponding adjusted *r*², constant, regression coefficient and *P* value, and the adjusted *r*² was used to compare the predictive accuracy. Patients were further divided into three groups according to the tertiles of LV/RV interventricular dyssynchrony—LSR-SD9. In addition, multivariable logistical regression modeling was used to analyze the association between interventricular dyssynchrony and risk assessment, described as odds ratios (ORs) and 95% confidence intervals (CIs). A receiver operator characteristic curve (ROC) was used to evaluate the predictive value of LSR-SD9 and identify the optimal cut-off point for risk assessment.

For 2D-STE measurement, intra- and interobserver variability were assessed for 20 randomly selected patients by the Bland-Altman method, and the results were described as follows: RV-GLS: $-0.13\% \pm 1.47\%$, 95% confidence interval (CI): -3.02% to 2.76% and $0.86\% \pm 1.29\%$, 95% CI: -1.67% to 3.40% , respectively; RV-SD6: 1.48 ± 6.37 ms, 95% CI: -10.99 to 13.96 ms and 3.08 ± 7.18 ms, 95% CI: -10.99 to 17.16 ms, respectively; LV-SD6: -0.43 ± 5.02 ms, 95% CI: -10.28 to 9.42 ms and 1.08 ± 5.50 ms, 95% CI: -9.70 to 11.87 ms, respectively; LSR-SD9: 0.88 ± 6.27 ms, 95% CI: -11.40 to 13.18 ms and 3.30 ± 7.87 ms, 95% CI: -12.14 to 18.73 ms, respectively; LR-SD6: 0.73 ± 7.51 ms, 95% CI: -13.99 to 15.46 ms and 1.19 ± 8.69 ms, 95% CI: -15.83 to 18.22 ms, respectively. These findings were similar to those of a previous study (20) and can be considered acceptable for our clinical purpose.

All statistical analyses were performed using SPSS software (version 19.0, IBM), GraphPad Prim software (version 6.01) and MedCalc (version 15.2). All statistical tests were two-sided, and *P*<0.05 was considered statistically significant.

Results

As described in *Table 1*, we recruited 66 PcPH patients (19 male and 47 female, 35 ± 13 years) for the present study, and

Table 1 Demographic, clinical, echocardiography and 2-dimensional speckle tracking echocardiography characteristics of the 66 pre-capillary PH patients

Characteristics	Number
Age (years)	35±13
Gender (male)	19 (28.8%)
BMI (kg/m ²)	22.58±3.91
Clinical characteristics	
WHO functional class	
I	8 (12.1%)
II	27 (40.9%)
III	31 (47%)
Laboratory examinations	
NT-proBNP (pg/mL)	1,113.97±1,264.82
NT-proBNP <300 pg/mL	23 (34.8%)
RDW (%)	14.23±1.92
BUN (mmol/L)	5.73±1.46
PO ₂ (mmHg)	73.29±20.29
Hemodynamics	
mPAP (mmHg)	54.03±13.94
CI (L/min/m ²)	3.16±0.84
PAWP (mmHg)	7.23±3.41
PVR (dyn·s·cm ⁻⁵)	779.66±288.26
mixed venous oxygen saturation (%)	70.21±5.46
Exercise capacity	
PVO ₂ (mL/min/kg)	13.97±3.61
6MWD (m)	409.22±107.74
Treatments	
PED-5i	54 (81.8%)
ERA	33 (50%)
PGI	5 (7.6%)
CCB	4 (6.1%)
Echocardiography characteristics	
LV function	
LVEF (%)	62.74±5.9
RV diastolic function	
E/A	1.45±0.62
E/E'	8.98±5.1
RV systolic function	
RV-FAC (%)	19.8±10.21
TAPSE (mm)	16.61±3.65
S' (cm/s)	10.44±2.25

Table 1 (continued)**Table 1** (continued)

Characteristics	Number
2D-STE characteristics	
RV-GLS (%)	-11.67±4.26
RV intraventricular dyssynchrony	
RV-SD6 (ms)	53.63±45.7
LV intraventricular dyssynchrony	
LV-SD6 (ms)	27.11±29.43
Interventricular dyssynchrony	
LSR-SD9 (ms)	55.18±39.79
LR-SD6 (ms)	42.08±34.82

Data are presented as mean ± standard deviation or counts (proportions). BMI, body mass index; NT-proBNP, N-terminal pro-brain natriuretic peptide; RDW, red cell distribution width; BUN, blood urea nitrogen; PO₂, oxygen partial pressure; mPAP, mean pulmonary arterial pressure; CI, cardiac index; PAWP, pulmonary artery wedge pressure; PVR, pulmonary vascular resistance; PED-5i, phosphodiesterase-5 inhibitors; ERA, endothelin-receptor antagonist; PGI, prostacyclin; CCB, calcium channel blockers; RV, right ventricular; FAC, fractional area change; LVEF, left ventricular ejection fraction; E, A, Doppler velocities of the trans-tricuspid flow; E', S', Doppler velocities of the tricuspid annulus; TAPSE, tricuspid annular plane systolic excursion. RV-GLS, RV global longitudinal strain; RV-SD6, the standard deviation (SD) of the corrected time intervals of the six segments of RV; LV-SD6, the SD of the corrected time intervals of the six segments of LV; LSR-SD9, the SD of the corrected time intervals of the nine segments including six segments of RV and three segments of LV free wall; LR-SD6, the SD of corrected time intervals of six segments including LV and RV free wall.

approximately 90% of the population was characterized as II-III (WHO-FC). In addition, linear correlation analyses showed that there were significant but relatively weak correlations between PVO₂ and WHO-FC ($r=-0.512$, $P<0.001$), NT-proBNP ($r=-0.493$, $P<0.001$), blood urea nitrogen (BUN, $r=-0.304$, $P=0.013$), oxygen partial pressure (PO₂, $r=-0.343$, $P=0.006$), E/E' ($r=-0.41$, $P=0.001$), and RV-FAC ($r=0.369$, $P=0.002$).

The first multivariate regression analysis considered clinical variables that significantly correlated with PVO₂ (WHO-FC, NT-proBNP, BUN, PO₂) and prognostic predictors suggested by previous studies, such as BMI (21) and red blood cell distribution width (RDW) (22,23), while echocardiographic parameters were excluded. Model-1 was constructed ($r^2=0.423$, $P<0.001$) and identified WHO-FC, NT-proBNP and BMI as independent predictors of PVO₂. The second analysis added conventional echocardiographic

Table 2 Multivariate linear regression analysis of echocardiographic and clinical variables associated with PVO₂

Variables	B	SE	β	P value	Adjusted r ²
Model-1					0.423
Intercept	26.311	2.423		<0.001	
WHO-FC	-1.862	0.566	-0.355	0.002	
NT-proBNP	-0.001	0.000	-0.399	0.001	
BMI	-0.295	0.091	-0.317	0.002	
Model-2					0.417
Intercept	23.037	2.806		<0.001	
WHO-FC	-2.592	0.543	-0.490	<0.001	
RV-FAC	10.758	3.725	0.296	0.006	
BMI	-0.221	0.094	-0.234	0.022	
Model-3					0.454
Intercept	20.805	2.926		<0.001	
WHO-FC	-2.174	0.557	-0.411	<0.001	
RV-GLS	-0.325	0.091	-0.375	0.001	
BMI	-0.241	0.091	-0.254	0.011	
Model-4					0.474
Intercept	26.358	2.424		<0.001	
WHO-FC	-2.542	0.513	-0.480	<0.001	
RV-SD6	-0.031	0.008	-0.379	<0.001	
BMI	-0.209	0.090	-0.221	0.024	
Model-5					0.483
Intercept	26.918	2.407		<0.001	
WHO-FC	-2.543	0.508	-0.481	<0.001	
LSR-SD9	-0.036	0.009	-0.389	<0.001	
BMI	-0.218	0.089	-0.231	0.017	

BMI, body mass index; NT-proBNP, N-terminal pro-brain natriuretic peptide; WHO-FC, WHO functional class; RV, right ventricular; FAC, fractional area change; RV-GLS, RV global longitudinal strain; RV-SD6, the standard deviation (SD) of the corrected time intervals of the six segments of RV; LSR-SD9, the SD of the corrected time intervals of the nine segments including six segments of RV and three segments of LV free wall.

parameters (E/E', RV-FAC) to the clinical variables and identified WHO-FC, RV-FAC and BMI as independent predictors of PVO₂ (Model-2, r²=0.417, P<0.001). Finally, we respectively added RV-GLS, RV-SD6, LV-SD6, LSR-SD9 and LR-SD6 to the conventional echocardiographic and clinical parameters, and identified RV-GLS (Model-3, r²=0.454, P=0.001), RV-SD6 (Model-4, r²=0.474, P<0.001) and LSR-SD9 (Model-5, r²=0.483, P<0.001) as independent predictors of PVO₂, and the predictive capability increased.

Of all the models constructed in our study, Model-5 including LSR-SD9 had the highest predictive capability for PVO₂ (Table 2).

To further evaluate the robustness of our results, the PH patients were divided into three groups based on the tertiles of LSR-SD9, and there were significant differences in PVO₂ and 6MWD among the three groups. As Figure 2 shows, the PVO₂ of the three groups in ascending order was 16.11±3.44, 13.99±3.54 and 11.80±2.49 mL/min/kg,

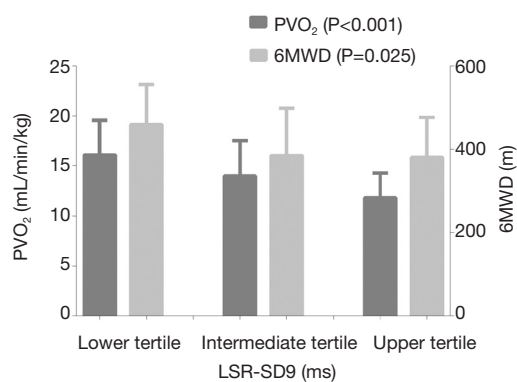


Figure 2 Histograms of PVO₂ and 6MWD distribution based on LV/RV interventricular dyssynchrony (LSR-SD9) tertiles. Means and interquartile ranges are displayed by boxes and whiskers. The three groups were based on the tertiles of LSR-SD9, and in ascending order. LV, left ventricular; RV, right ventricular; PVO₂, peak oxygen consumption (mL/min/kg); 6MWD, six-minute walk distance (m).

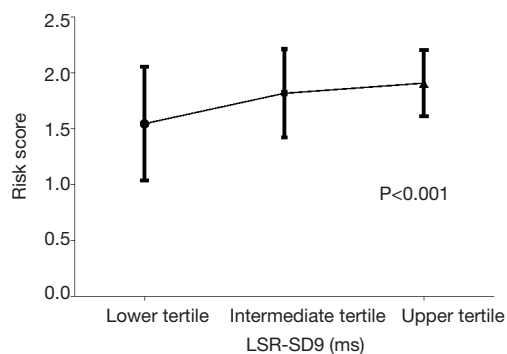


Figure 3 The differences of risk scores (according to 2015 ESC Guidelines, 1 point represents low risk, and 2 points represent moderate-high risk) based on interventricular dyssynchrony (LSR-SD9) tertiles distribution. The three groups were based on the tertiles of LSR-SD9, and in ascending order.

respectively ($P<0.001$); while the 6MWD was 458.64 ± 96.5 , 385.05 ± 113.64 and 380.25 ± 96.11 m, respectively ($P=0.025$). The risk scores of the comprehensive risk assessment according to the 2015 ESC Guidelines are shown in *Figure 3* (lower tertile *vs.* intermediate tertile *vs.* upper tertile: 1.55 ± 0.51 *vs.* 1.82 ± 0.4 *vs.* 1.91 ± 0.29 ; $P<0.001$). In other words, the worse the degree of interventricular dyssynchrony, the worse the exercise capacity and the higher the 1-year mortality risk.

Among the 66 PcPH patients in the present study,

Table 3 Logistic regression models for risk assessment in 66 pre-capillary pulmonary hypertension patients

Characteristic	OR ¹	95% CI	P value
Model-1			
LSR-SD9	1.027	1.003–1.052	0.030
Age	1.021	0.965–1.080	0.469
Male sex	0.875	0.228–3.370	0.864
BMI	1.026	0.862–1.223	0.770
Model-2			
RV-SD6	1.019	0.999–1.039	0.059
Age	1.016	0.962–1.073	0.564
Male sex	0.801	0.214–3.002	0.742
BMI	1.036	0.873–1.229	0.686

N=66; 16 low risk and 50 intermediate-high risk. ¹, OR, per 1 ms increases in LSR-SD9 and RV-SD6, 1-year increases in age, and 1 kg/m² increases in BMI. CI, confidence interval; BMI, body mass index; RV, right ventricular; RV-SD6, the standard deviation (SD) of the corrected time intervals of the six segments of RV; LSR-SD9, the SD of the corrected time intervals of the nine segments including six segments of RV and three segments of LV free wall.

16 patients met the criteria for low-risk classification according to the 2015 ESC guidelines. Logistic regression showed that after adjusting for age, sex and BMI, LSR-SD9 was independently associated with risk assessment (OR 1.027, 95% CI: 1.003–1.052, $P=0.03$), and the results are shown in *Table 3*. The ROC curve of LSR-SD9 for the prediction of low risk classification is shown in *Figure 4*, and the area under the curve was 0.73 ($P=0.006$). The optimal cut-off point of LSR-SD9 was 27.53 ms, which had 84.0% sensitivity and 62.5% specificity for the prediction of risk classification in PH patients.

Discussion

The present study, to the best of our knowledge, was the first time to propose the conception of 2D-STE-detected interventricular dyssynchrony and showed that interventricular dyssynchrony contributed to a better evaluation of impaired exercise capacity and disease severity in PcPH patients; compared with RV intraventricular dyssynchrony, the predictive capability of interventricular dyssynchrony tended to be stronger. Additionally, this added predictive value was not observed for LV intraventricular

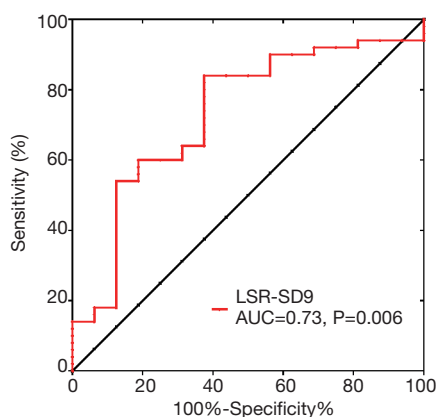


Figure 4 Receiver operator characteristic curve of LSR-SD9 for the prediction of risk assessment in pre-capillary PH patients. LSR-SD9: the SD of the corrected time intervals of the nine segments including six segments of RV and three segments of LV free wall. LV, left ventricular; RV, right ventricular; PH, pulmonary hypertension; SD, standard deviation.

dyssynchrony.

We mainly focused on interventricular dyssynchrony in our study, because LV dysfunction was commonly observed in PH patients but has not previously received sufficient attention, and its mechanisms remain unclear. From the macroscopic point of view, LV dysfunction in PH patients may develop due to a preload-dependent pathway. Kallianos *et al.* reported a relationship between RV end diastolic volume index (RVEDVI) and septal strain measured by CMR in PH patients, suggesting that ventricular interdependent was a possible mechanism of LV dysfunction before a significant decline of LVEF in this population (16). Additionally, several studies have demonstrated that the septum deformity caused by high pressure of RV may be responsible for LV contractile dysfunction in PAH patients with preserved or mildly depressed LVEF (24,25). At the micro level, Sharma *et al.* showed that pyruvate dehydrogenase-4 (PDK4) and B-MHC levels expressed by LV changed during RV remodeling induced by hypoxia (26); Lourenço *et al.* reported an upregulation of endothelin-1 mRNA in the left ventricle in a hypoxia/monocrotaline-induced PAH model, which was also observed in the context of impaired LV function (27). Research by Imai *et al.* showed some pathological molecular pathways activated in the RV myocardium in a transverse aortic constriction-induced short-term LV pressure-overload model, such as increased levels of brain natriuretic peptide (BNP) mRNA, interleukin-1 beta (IL-1b) and interleukin-6

(IL-6) and increased calcineurin activity, suggesting that RV-LV interventricular interaction might be mediated by inflammatory activity (28). For CTD-PAH patients, LV dyssynchrony may be a direct consequence of primary myocardial involvement, subsequent to the concurrent increases in pulmonary arterial pressures (29,30); and the pathological mechanism underlying LV dyssynchrony may include decreased capillary density, increased apoptosis of endothelial cells, perivascular inflammation, collagen deposition and myocardial fibrosis (31). All these studies suggested that simultaneous LV dysfunction was inevitable in patients with PH as the disease progressed.

PcPH originates as a primary pathology of the pulmonary vasculature (32), which causes a persistently increased RV afterload. RV myocytes are characterized by the longitudinal inflow (proximal) and circumferential outflow (distal) (33), but predominantly oriented longitudinally so that RV contraction primarily results in longitudinal shortening (34). Therefore, RV dyssynchrony based on longitudinal strain measured by 2D-STE corresponded to RV contractile function and was thereby associated with cardiac output (CO) and exercise capacity, as demonstrated in our study and a previous study (11). A possible pathophysiological explanation of this phenomenon is that patients with severe PH often have slower blood flow from the right to the left side of the heart and the coupled LV dyssynchrony further reduces the CO of the left ventricle. Then, this process is gradually accentuated during exercise, which adds to the decrease in both right and LV CO, eventually leading to impaired exercise capacity (35).

The 2015 ESC risk assessment strategy was used to evaluate disease severity in PH patients; however, the assessment was comprehensive and included invasive methods such as RHC. Furthermore, there were no detailed recommendations about management in the context of combinations of different risk stratification parameters. We considered a patient to have low risk only if he or she met all criteria indicating low risk in clinical practice; otherwise, changes in treatment should be considered. Rehman *et al.* showed that RV global and free-wall longitudinal strain identified by 2D-STE might classify PAH patients according to exercise testing risk stratification cut-offs, but the parameters of intra- and interventricular dyssynchrony were not mentioned. They also found that none of the echocardiographic LV parameters had the same ability, which may be due to their exclusion of all patients with LV dysfunction from their study groups (36). In contrast, research from Nakano indicated that the evaluations of both

LV and RV functions were of great importance for PAH and CTEPH patients, but they used standard echocardiography rather than 2D-STE parameters to evaluate the LV and RV functions (37). In the present study, we found that interventricular dyssynchrony may be a noninvasive and convenient indicator for risk stratification of PcPH patients. 2D-STE-detected LV/RV inter- and intraventricular dyssynchrony could be a routine measurement that could contribute to the assessment of severity and therapeutic strategies for PcPH patients in the future.

Notably, compared with RV intraventricular dyssynchrony, the interventricular dyssynchrony described by LSR-SD9 may have a slightly stronger value for predicting PVO₂ and risk assessment. In other words, LV dysfunction is inevitable during disease progression, and comprehensive analyses of the left and right heart functions may be superior to the analysis of right heart function alone, even in PH patients who are thought to present with predominantly RV dysfunction. These findings were not surprising, and were supported by a previous study in a similar group of patients (38). Therefore, early identification of biventricular dysfunction in clinical practice may help clinicians assess disease severity and prognosis more accurately and in a timely manner, which further contributes to determining therapeutic strategies and optimizing the time to heart/lung transplantation, ultimately benefiting PH patients.

There were also some limitations in our study. First, as a single center study, the sample size was relatively small, but considering a relatively rare disease was being explored, the sample size was acceptable. Second, although we performed all the echocardiographic measurements according to the guidelines, there was inevitable heterogeneity and variability of the quality of echocardiography and 2D speckle-tracking parameters. To improve the data quality, all of the measurements were performed in strict accordance with the guidelines, and the intra- and interobserver variability were considered acceptable for our clinical purpose. Third, for a few patients in our study, echocardiography and RHC were not performed simultaneously, which was described in the Methods section, which may have had little or no influence on our results. Finally, this was a cross-sectional study; no cause-effect relationships were demonstrated, and regular follow-up will be performed in the future.

Conclusions

In conclusion, interventricular dyssynchrony detected by

2D-STE contributed to a better evaluation of exercise capacity and disease severity in PcPH patients.

Acknowledgments

We are indebted to the patients who participated in this study. We thank the research staff, the Department staff of Ultrasound for their most valuable efforts.

Funding: The present study was supported by the grant of Capital Health Development and Scientific Research Projects (2016–2-4036), CAMS Initiative for Innovative Medical (2016-I2M-3-006) and the Biomedicine and Life Sciences Innovation Cultivation Research Project (Z161100000116052).

Footnote

Conflicts of Interest: All authors have completed the ICMJE uniform disclosure form (available at <http://dx.doi.org/10.21037/atm.2020.03.146>). The authors have no conflicts of interest to declare.

Ethical Statement: The authors are accountable for all aspects of the work in ensuring that questions related to the accuracy or integrity of any part of the work are appropriately investigated and resolved. The present study was complied with the 1975 Declaration of Helsinki and was approved by the Ethics Committee of Fuwai Hospital (No. 2018-1063). All participants signed their written informed consent.

Open Access Statement: This is an Open Access article distributed in accordance with the Creative Commons Attribution-NonCommercial-NoDerivs 4.0 International License (CC BY-NC-ND 4.0), which permits the non-commercial replication and distribution of the article with the strict proviso that no changes or edits are made and the original work is properly cited (including links to both the formal publication through the relevant DOI and the license). See: <https://creativecommons.org/licenses/by-nc-nd/4.0/>.

References

1. Vonk-Noordegraaf A, Haddad F, Chin KM, et al. Right heart adaptation to pulmonary arterial hypertension: physiology and pathobiology. *J Am Coll Cardiol* 2013;62:D22-33.
2. Kasner M, Westermann D, Steendijk P, et al. Left

- ventricular dysfunction induced by nonsevere idiopathic pulmonary arterial hypertension: a pressure-volume relationship study. *Am J Respir Crit Care Med* 2012;186:181-9.
3. Saleh S, Liakopoulos OJ, Buckberg GD. The septal motor of biventricular function. *Eur J Cardiothorac Surg* 2006;29 Suppl 1:S126-38.
 4. Benza RL, Miller DP, Gomberg-Maitland M, et al. Predicting survival in pulmonary arterial hypertension: insights from the Registry to Evaluate Early and Long-Term Pulmonary Arterial Hypertension Disease Management (REVEAL). *Circulation* 2010;122:164-72.
 5. Arena R, Lavie CJ, Milani RV, et al. Cardiopulmonary exercise testing in patients with pulmonary arterial hypertension: an evidence-based review. *J Heart Lung Transplant* 2010;29:159-73.
 6. Galiè N, Humbert M, Vachiery JL, et al. 2015 ESC/ERS Guidelines for the diagnosis and treatment of pulmonary hypertension: The Joint Task Force for the Diagnosis and Treatment of Pulmonary Hypertension of the European Society of Cardiology (ESC) and the European Respiratory Society (ERS): Endorsed by: Association for European Paediatric and Congenital Cardiology (AEPC), International Society for Heart and Lung Transplantation (ISHLT). *Eur Respir J* 2015;46:903-75.
 7. Wensel R, Opitz CF, Anker SD, et al. Assessment of survival in patients with primary pulmonary hypertension: importance of cardiopulmonary exercise testing. *Circulation* 2002;106:319-24.
 8. Blumberg FC, Arzt M, Lange T, et al. Impact of right ventricular reserve on exercise capacity and survival in patients with pulmonary hypertension. *Eur J Heart Fail* 2013;15:771-5.
 9. Marcadet DM. Exercise testing: New guidelines. *Presse Med* 2019;48:1387-92.
 10. Badagliacca R, Reali M, Poscia R, et al. Right Intraventricular Dyssynchrony in Idiopathic, Heritable, and Anorexigen-Induced Pulmonary Arterial Hypertension: Clinical Impact and Reversibility. *JACC Cardiovasc Imaging* 2015;8:642-52.
 11. Badagliacca R, Papa S, Valli G, et al. Right ventricular dyssynchrony and exercise capacity in idiopathic pulmonary arterial hypertension. *Eur Respir J* 2017. doi: 10.1183/13993003.01419-2016.
 12. Liu BY, Wu WC, Zeng QX, et al. Two-dimensional speckle tracking echocardiography assessed right ventricular function and exercise capacity in pre-capillary pulmonary hypertension. *Int J Cardiovasc Imaging* 2019;35:1499-508.
 13. Park JH, Kusunose K, Kwon DH, et al. Relationship between Right Ventricular Longitudinal Strain, Invasive Hemodynamics, and Functional Assessment in Pulmonary Arterial Hypertension. *Korean Circ J* 2015;45:398-407.
 14. Motoki H, Borowski AG, Shrestha K, et al. Right ventricular global longitudinal strain provides prognostic value incremental to left ventricular ejection fraction in patients with heart failure. *J Am Soc Echocardiogr* 2014;27:726-32.
 15. Cheng XL, Liu BY, Wu WC, et al. Impact of right ventricular dyssynchrony on prognosis of patients with idiopathic pulmonary arterial hypertension. *Pulm Circ* 2019;9:2045894019883609.
 16. Kallianos K, Brooks GC, Mukai K, et al. Cardiac Magnetic Resonance Evaluation of Left Ventricular Myocardial Strain in Pulmonary Hypertension. *Acad Radiol* 2018;25:129-35.
 17. Liu BY, Wu WC, Zeng QX, et al. EXPRESS: Left ventricular early diastolic strain rate detected by two-dimensional speckle tracking echocardiography and disease severity in pre-capillary pulmonary hypertension. *Pulm Circ* 2019. [Epub ahead of print].
 18. Rudski LG, Lai WW, Afilalo J, et al. Guidelines for the echocardiographic assessment of the right heart in adults: a report from the American Society of Echocardiography endorsed by the European Association of Echocardiography, a registered branch of the European Society of Cardiology, and the Canadian Society of Echocardiography. *J Am Soc Echocardiogr* 2010;23:685-713; quiz 786-8.
 19. Bazett HC. An analysis of the time-relations of electrocardiograms. *Heart* 1920;353-70.
 20. Kalogeropoulos AP, Georgiopoulou VV, Howell S, et al. Evaluation of right intraventricular dyssynchrony by two-dimensional strain echocardiography in patients with pulmonary arterial hypertension. *J Am Soc Echocardiogr* 2008;21:1028-34.
 21. Hu EC, He JG, Liu ZH, et al. Survival advantages of excess body mass index in patients with idiopathic pulmonary arterial hypertension. *Acta Cardiol* 2014;69:673-8.
 22. Abul Y, Ozsu S, Korkmaz A, et al. Red cell distribution width: a new predictor for chronic thromboembolic pulmonary hypertension after pulmonary embolism. *Chron Respir Dis* 2014;11:73-81.
 23. Rhodes CJ, Wharton J, Howard LS, et al. Red cell distribution width outperforms other potential circulating

- biomarkers in predicting survival in idiopathic pulmonary arterial hypertension. *Heart* 2011;97:1054-60.
24. Puwanant S, Park M, Popovic ZB, et al. Ventricular geometry, strain, and rotational mechanics in pulmonary hypertension. *Circulation* 2010;121:259-66.
 25. Hardegree EL, Sachdev A, Fenstad ER, et al. Impaired left ventricular mechanics in pulmonary arterial hypertension: identification of a cohort at high risk. *Circ Heart Fail* 2013;6:748-55.
 26. Sharma S, Taegtmeier H, Adroque J, et al. Dynamic changes of gene expression in hypoxia-induced right ventricular hypertrophy. *Am J Physiol Heart Circ Physiol* 2004;286:H1185-92.
 27. Lourenço AP, Roncon-Albuquerque R Jr, Brás-Silva C, et al. Myocardial dysfunction and neurohumoral activation without remodeling in left ventricle of monocrotaline-induced pulmonary hypertensive rats. *Am J Physiol Heart Circ Physiol* 2006;291:H1587-94.
 28. Imai Y, Kariya T, Iwakiri M, et al. Sildenafil ameliorates right ventricular early molecular derangement during left ventricular pressure overload. *Plos One* 2018;13:e0195528.
 29. Guerra F, Stronati G, Fischietti C, et al. Global longitudinal strain measured by speckle tracking identifies subclinical heart involvement in patients with systemic sclerosis. *Eur J Prev Cardiol* 2018;25:1598-606.
 30. Fowler RM, Maiorana AJ, Jenkins SC, et al. A comparison of the acute haemodynamic response to aerobic and resistance exercise in subjects with exercise-induced pulmonary arterial hypertension. *Eur J Prev Cardiol* 2013;20:605-12.
 31. Venalis P, Kumanovics G, Schulze-Koops H, et al. Cardiomyopathy in murine models of systemic sclerosis. *Arthritis Rheumatol* 2015;67:508-16.
 32. Simonneau G, Robbins IM, Beghetti M, et al. Updated clinical classification of pulmonary hypertension. *J Am Coll Cardiol* 2009;54:S43-54.
 33. Lang RM, Badano LP, Tsang W, et al. EAE/ASE recommendations for image acquisition and display using three-dimensional echocardiography. *Eur Heart J Cardiovasc Imaging* 2012;13:1-46.
 34. Ho SY, Nihoyannopoulos P. Anatomy, echocardiography, and normal right ventricular dimensions. *Heart* 2006;92 Suppl 1:i2-13.
 35. Popovic D, Arena R, Guazzi M. A flattening oxygen consumption trajectory phenotypes disease severity and poor prognosis in patients with heart failure with reduced, mid-range, and preserved ejection fraction. *Eur J Heart Fail* 2018;20:1115-24.
 36. Rehman MB, Garcia R, Christiaens L, et al. Power of resting echocardiographic measurements to classify pulmonary hypertension patients according to European society of cardiology exercise testing risk stratification cut-offs. *Int J Cardiol* 2018;257:291-7.
 37. Nakano Y, Okumura N, Adachi S, et al. Left ventricular end-diastolic dimension and septal e' are predictors of cardiac index at rest, while tricuspid annular plane systolic excursion is a predictor of peak oxygen uptake in patients with pulmonary hypertension. *Heart Vessels* 2018;33:521-8.
 38. Henein MY, Gronlund C, Tossavainen E, et al. Right and left heart dysfunction predict mortality in pulmonary hypertension. *Clin Physiol Funct Imaging* 2017;37:45-51.

Cite this article as: Liu BY, Wu WC, Zeng QX, Liu ZH, Niu LL, Tian Y, Cheng XL, Luo Q, Zhao ZH, Huang L, Wang H, He JG, Xiong CM. Two-dimensional speckle tracking echocardiography detected interventricular dyssynchrony predicts exercise capacity and disease severity in pre-capillary pulmonary hypertension. *Ann Transl Med* 2020;8(7):456. doi: 10.21037/atm.2020.03.146